XVII Mexican Workshop on Particles and Fields (MWPF)

Phenomenological analysis in direct photon production using Neural Network

David Francisco Rentería-Estrada
Universidad Autónoma de Sinaloa, México

In colaboration with:
Roger J. Hernández Pinto
German F.R. Sborlini
Pia Zurita

Based on:
- 1011.0486
- 2104.14663
- 2112.05043

November 21th, 2022

Process

In this work we are interested in studying the production of a direct photon plus a pion in proton-proton collision:

$$pp \rightarrow \pi^{+} + \gamma$$

The aim is reconstruct the momentum fraction $\mathbf{x_1}$, $\mathbf{x_2}$ and $\mathbf{z}$ of the originals partons in the interaction to NLO QCD + LO QED accuracy .

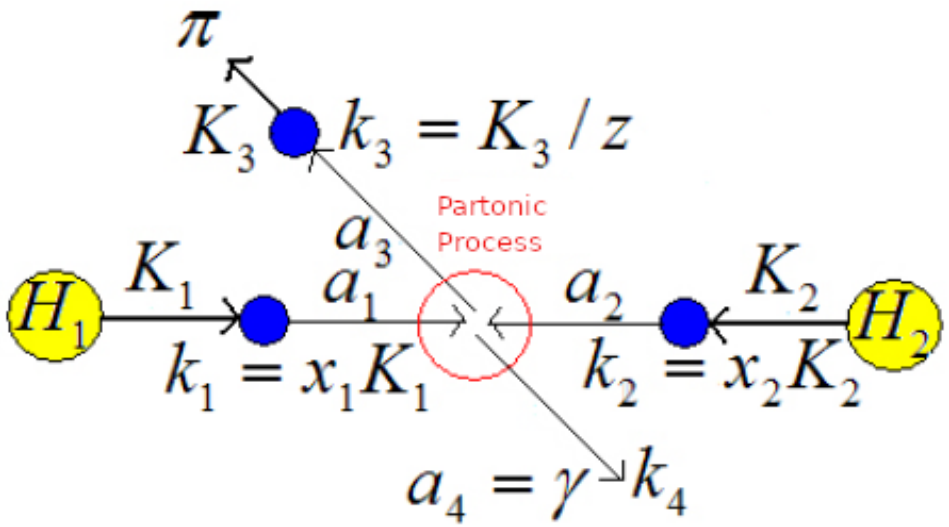

direc photon

Motivation

- Aim: reconstruct the momentum fractions x_1, x_2 and z.

- Nowadays, Machine Learning is a tool that allows to make a predictive model to reconstruct $\{x_1, x_2, z\}$.

1011.0486

PHYSICAL REVIEW D **83,** 074022 (2011)

Hadron plus photon production in polarized hadronic collisions at next-to-leading order accuracy

Daniel de Florian and Germán F. R. Sborlini

Departamento de Física Facultad de Ciencias Exactas y Naturales, Universidad de Buenos Aires Pabellón I, Ciudad Universitaria (1428) Capital Federal, Argentina

(Received 3 November 2010; revised manuscript received 23 February 2011; published 27 April 2011)

We compute the next-to-leading order QCD corrections to the polarized (and unpolarized) cross sections for the production of a hadron accompanied by an opposite-side prompt photon. This process, being studied at RHIC, permits us to reconstruct partonic kinematics using experimentally measurable variables. We study the correlation between the reconstructed momentum fractions and the true partonic ones, which in the polarized case might allow us to reveal the spin-dependent gluon distribution with a higher precision.

DOI: 10.1103/PhysRevD.83.074022 PACS numbers: 13.88.+e, 12.38.Bx, 13.87.Fh

2011

2104.14663

symmetry 2021 MDPI

Article

Analysis of the Internal Structure of Hadrons Using Direct Photon Production

David Francisco Rentería-Estrada [1,†], Roger José Hernández-Pinto [1,*,†] and German Sborlini [2,3,†]

1 Facultad de Ciencias Físico-Matemáticas, Universidad Autónoma de Sinaloa, Ciudad Universitaria, CP 80000 Culiacán, Mexico; davidrenteria.fcfm@uas.edu.mx
2 Instituto de Física Corpuscular, Universitat de València—Consejo Superior de Investigaciones Científicas, Parc Científic, E-46980 Paterna, Spain; german.sborlini@desy.de

2112.05043

SciPost SciPost Phys. Core 5, 049 (2022)

Reconstructing partonic kinematics at colliders with machine learning

David F. Rentería Estrada[1⋆], Roger J. Hernández-Pinto[1], German F. R. Sborlini[2,3] and Pia Zurita[4]

1 Facultad de Ciencias Físico-Matemáticas, Universidad Autónoma de Sinaloa, Ciudad Universitaria, CP 80000 Culiacán, Mexico
2 Deutsches Elektronen-Synchrotron DESY, Platanenallee 6, 15738 Zeuthen, Germany
3 Departamento de Física Fundamental e IUFFyM, Universidad de Salamanca, E-37008 Salamanca, Spain
4 Institut für Theoretische Physik, Universität Regensburg, 93040 Regensburg, Germany

⋆ davidrenteria.fcfm@uas.edu.mx

for deciphering there are several to complement onstraints from nternal structure ron plus photon neasurements.

2022

Hadronic Cross–Section

In hadron-hadron collisions, the cross section is described by the convolution between PDFs, FFs, and the partonic cross section.

$$d\sigma^{h_1 h_2 \to HX} = \sum_{a,b,c} \int_0^1 dx \int_0^1 dy \int_0^1 dz \, f_a^{h_1}(x,\mu_I) f_b^{h_2}(y,\mu_I) d_c^H(z,\mu_F) d\hat{\sigma}_{ab\to cX}$$

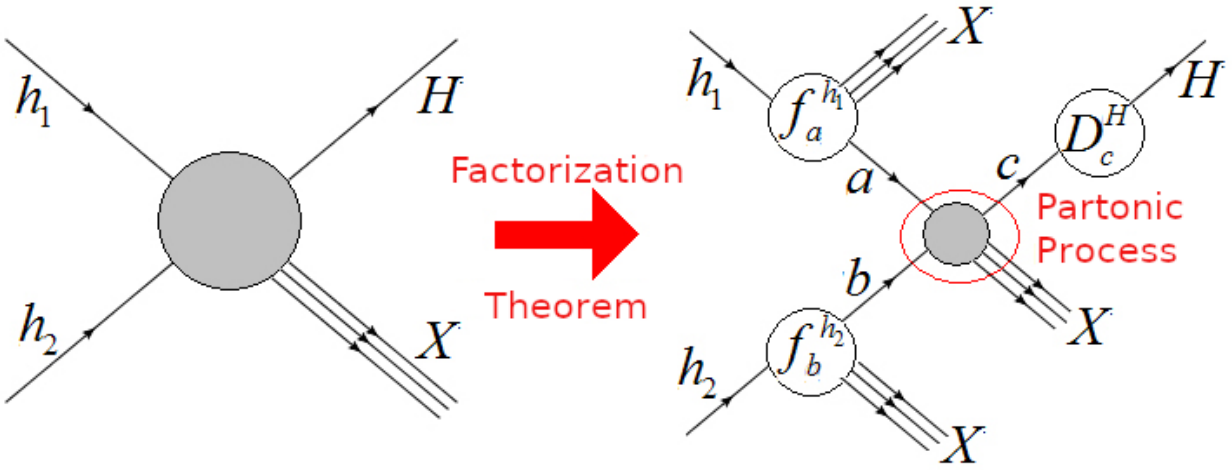

Cross section calculation

- The Cross-Section at NLO QCD is implement in FKS (virtual + real + UV counter terms + ISR counter-terms)

Hadronic cross-section

$$d\sigma_{H_1H_2\to h\gamma} = \sum_{a_1,a_2,a_3}\int_0^1 dx_1\,dx_2\,dz\, f_{a_1}^{H_1}(x_1,\mu_I) f_{a_2}^{H_2}(x_2,\mu_I) d_{a_3}^{h}(z,\mu_F) d\hat{\sigma}^{ISO}_{a_1a_2\to a_3\gamma}.$$

Partonic cross-section

$$\begin{aligned} d\hat{\sigma}^{\rm ISO}_{a_1\,a_2\to a_3\,\gamma} &= \frac{\alpha_s}{2\pi}\frac{\alpha}{2\pi}\int d{\rm PS}^{2\to 2}\,\frac{|\mathcal{M}^{(0)}|^2(x_1K_1,x_2K_2,K_3/z,K_4)}{2\hat{s}}\,\mathcal{S}_2 \\ &+ \frac{\alpha_s^2}{4\pi^2}\frac{\alpha}{2\pi}\int d{\rm PS}^{2\to 2}\,\frac{|\mathcal{M}^{(1)}|^2(x_1K_1,x_2K_2,K_3/z,K_4)}{2\hat{s}}\,\mathcal{S}_2 \\ &+ \frac{\alpha_s^2}{4\pi^2}\frac{\alpha}{2\pi}\sum_{a_5}\int d{\rm PS}^{2\to 3}\,\frac{|\mathcal{M}^{(0)}|^2(x_1K_1,x_2K_2,K_3/z,K_4,k_5)}{2\hat{s}}\,\mathcal{S}_3 \end{aligned}$$

$$d\hat{\sigma}^{\rm ISO,QED}_{a_1\,a_2\to a_3\,\gamma} = \frac{\alpha^2}{4\pi^2}\int d{\rm PS}^{2\to 2}\,\frac{|\mathcal{M}^{(0)}_{QED}|^2(x_1K_1,x_2K_2,K_3/z,K_4)}{2\hat{s}}\,\mathcal{S}_2.$$

LO QCD	LO QED	NLO QCD
$q\bar{q}\to\gamma g$	$q\gamma\to\gamma q$	$q\bar{q}\to\gamma gg$
$qg\to\gamma q$	$q\bar{q}\to\gamma\gamma$.	$qg\to\gamma gq$
		$gg\to\gamma q\bar{q}$
		$q\bar{q}\to\gamma Q\bar{Q}$
		$qQ\to\gamma qQ$

Computational details

The selection procedure is given by the Smooth Cone Isolation algorithm

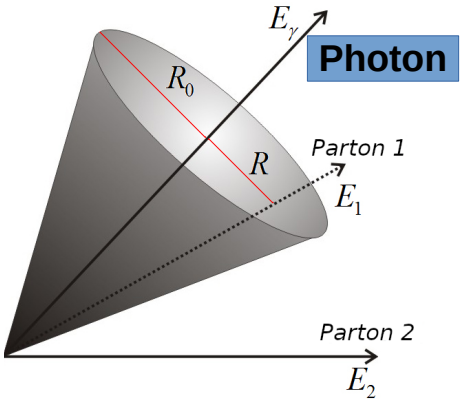

$$R = r_j = \sqrt{(\eta_j - \eta_0)^2 + (\phi_j - \phi_0)^2}$$

Smooth cone isolation

Computational details

The selection procedure is given by the Smooth Cone Isolation algorithm

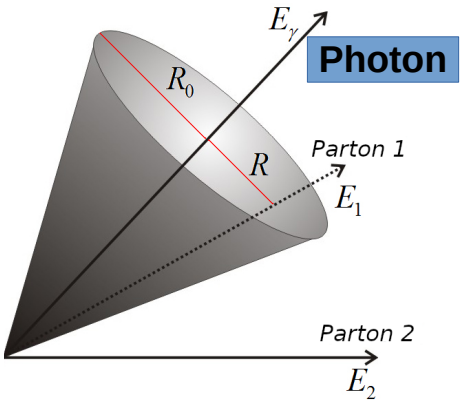

$$R = r_j = \sqrt{(\eta_j - \eta_0)^2 + (\phi_j - \phi_0)^2}$$

Smooth cone isolation

Smooth function: $\xi(r) = \epsilon_\gamma E_T^\gamma \left(\frac{1-\cos(r)}{1-\cos r_0} \right)^4$

Selection criteria

Define: $\mathrm{E}_T(r) = \sum_j E_{T_j} \Theta(r - r_j)$

If $\mathrm{E}_T(r) < \xi(r)$ Then:

γ is Isolated

Else:

γ is not Isolated

Computational details

The selection procedure is given by the Smooth Cone Isolation algorithm

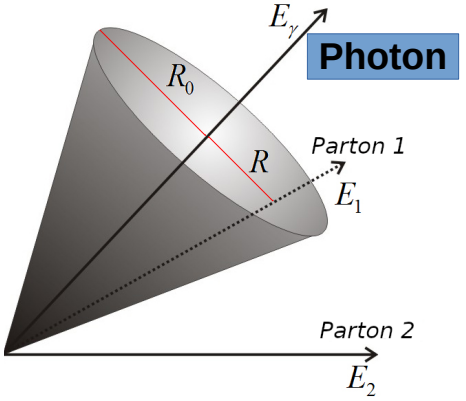

$$R = r_j = \sqrt{(\eta_j - \eta_0)^2 + (\phi_j - \phi_0)^2}$$

Smooth cone isolation

Smooth function: $\xi(r) = \epsilon_\gamma E_T^\gamma \left(\frac{1-\cos(r)}{1-\cos r_0} \right)^4$

Selection criteria

Define: $\mathrm{E}_T(r) = \sum_j E_{T_j} \Theta(r - r_j)$

If $\mathrm{E}_T(r) < \xi(r)$ Then:

γ is Isolated

Else:

γ is not Isolated

The cuts are used by STAR/PHENIX @ RHIC

$$|\eta^h| \leq 0.35\,, \quad |\eta^\gamma| \leq 0.35\,, \quad p_T^h \geq 2\,\mathrm{GeV}\,, \quad 5\,\mathrm{GeV} \leq p_T^\gamma \leq 15\,\mathrm{GeV}$$

First: Photon + Hadron distributions

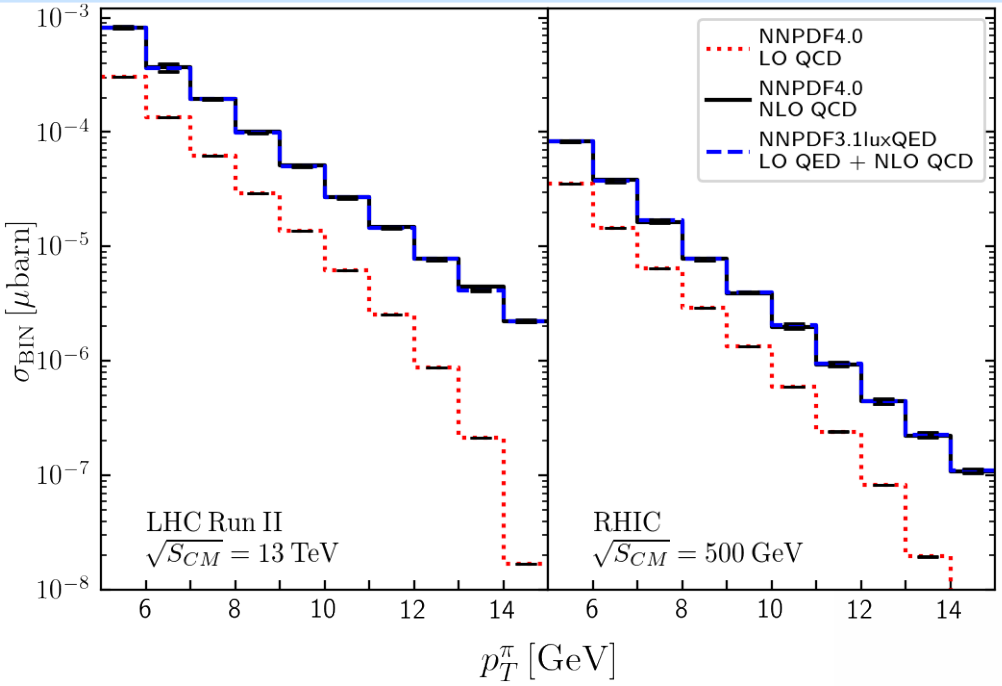

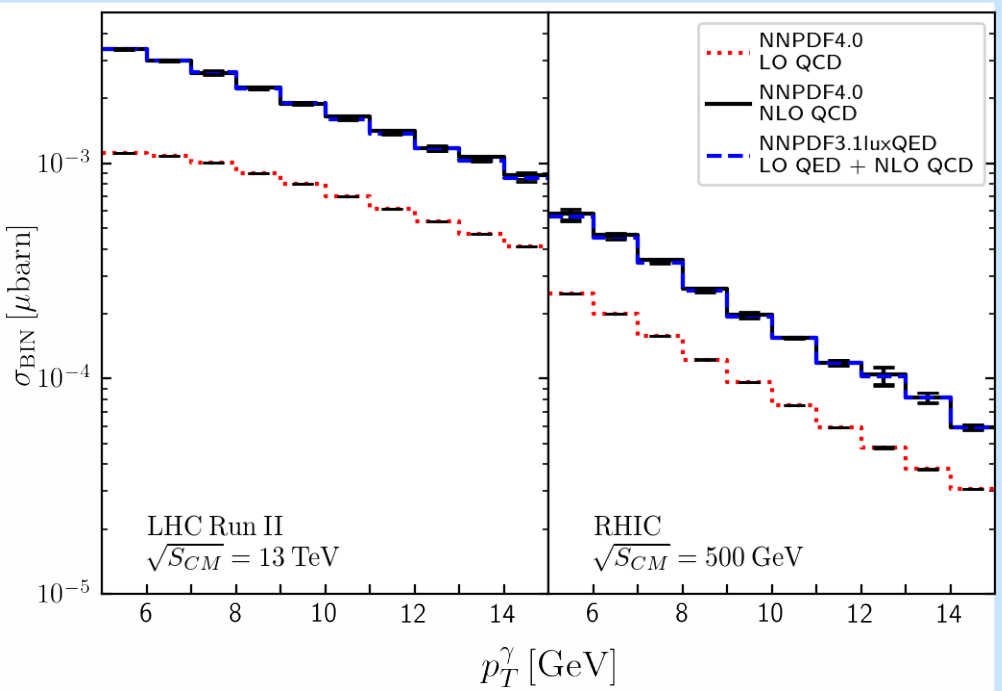

2112.05043 [hep-ph]

Transverse momentum distribution.

- The cross-section increases for higher c.m. energies.
- The distribution in p_T^{π} falls faster than the p_T^{γ} -spectrum, mainly because of the convolution with the FFs.

First: Photon + Hadron distributions

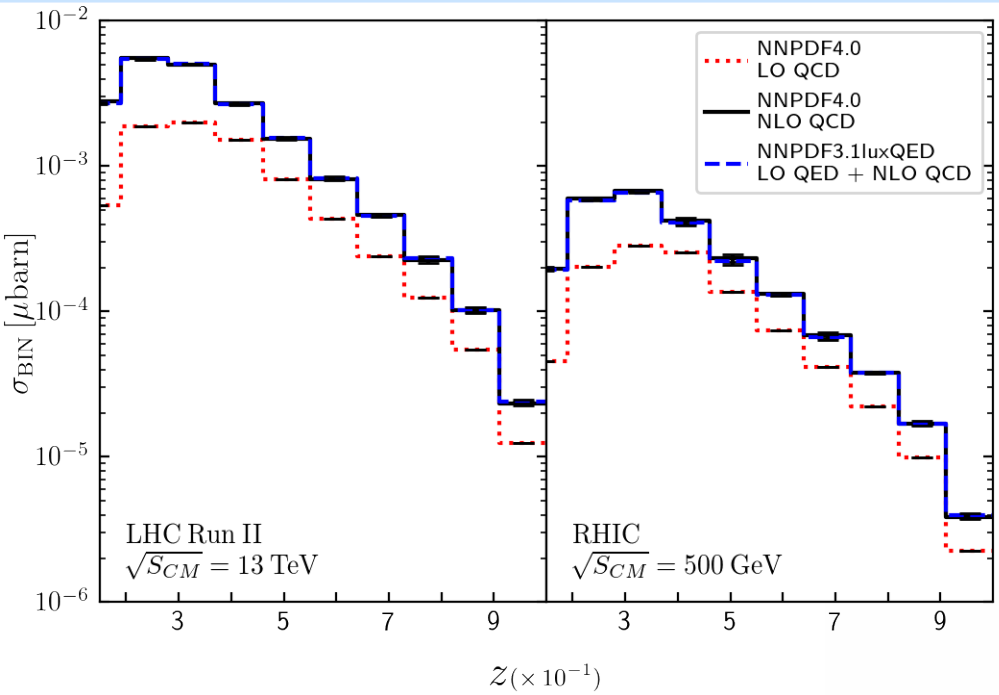

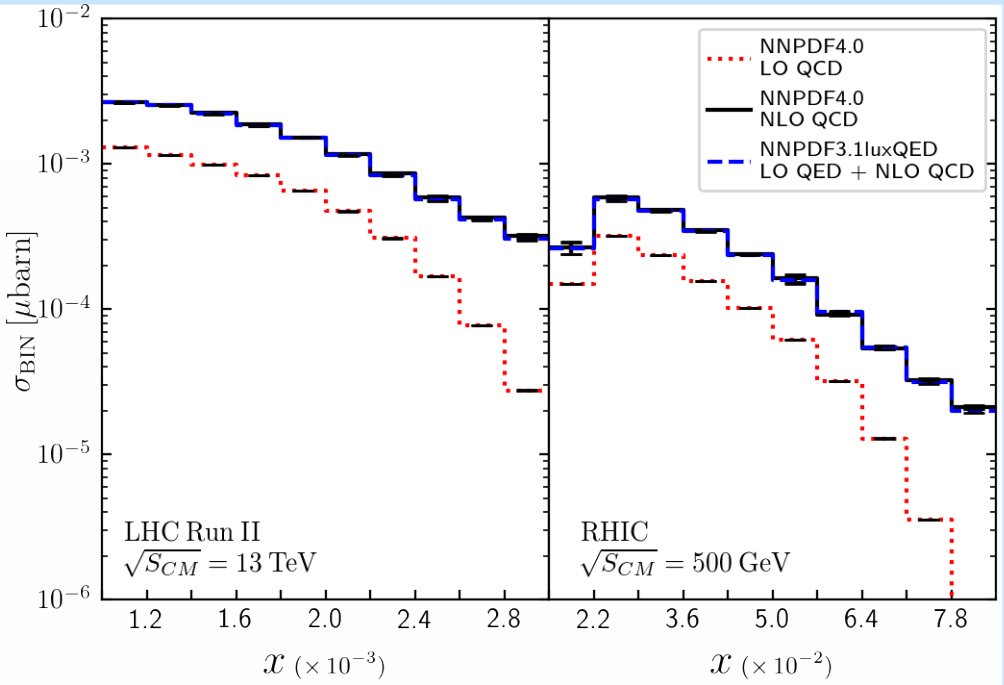

Fraction momentum distribution.

2112.05043 [hep-ph]

- Important NLO QCD corrections, but small percent-level LO QED ones.
- The experimental cut in p_T^γ induces a restriction on the maximum value of ***x*** involved in the collision.
- The distribution present a peak, located at $\mathbf{z_{Peak}} \approx 0.35$ for RHIC $\mathbf{z_{Peak}} \approx 0.25$ for LHC Run II.

Reconstructing the partonic kinematics

Experimentally accessible quantities:

$$\bar{\mathcal{V}}_{\rm Exp} = \{\bar{p}_T^{\gamma}, \bar{p}_T^{\pi}, \bar{\eta}^{\gamma}, \bar{\eta}^{\pi}, \overline{\cos}(\phi^{\pi} - \phi^{\gamma})\}$$ ← Detector measurements

Exactly solutions at LO accuracy

$$x_{1,2} = \frac{p_T^{\gamma}}{\sqrt{s}}\left(e^{\eta^{\pm\pi}} + e^{\eta^{\pm\gamma}}\right) \qquad z = \frac{p_T^{\pi}}{p_T^{\gamma}}$$

Approximation solutions at NLO QCD accuracy

$$X_{1,\rm REC} = \frac{p_T^{\gamma}\exp(\eta^{\pi}) - \cos(\phi^{\pi} - \phi^{\gamma})\, p_T^{\gamma}\exp(\eta^{\gamma})}{\sqrt{S_{CM}}}$$

$$X_{2,\rm REC} = \frac{p_T^{\gamma}\exp(-\eta^{\pi}) - \cos(\phi^{\pi} - \phi^{\gamma})\, p_T^{\gamma}\exp(-\eta^{\gamma})}{\sqrt{S_{CM}}}$$

$$Z_{\rm REC} = -\cos(\phi^{\pi} - \phi^{\gamma})\frac{p_T^{\pi}}{p_T^{\gamma}}$$

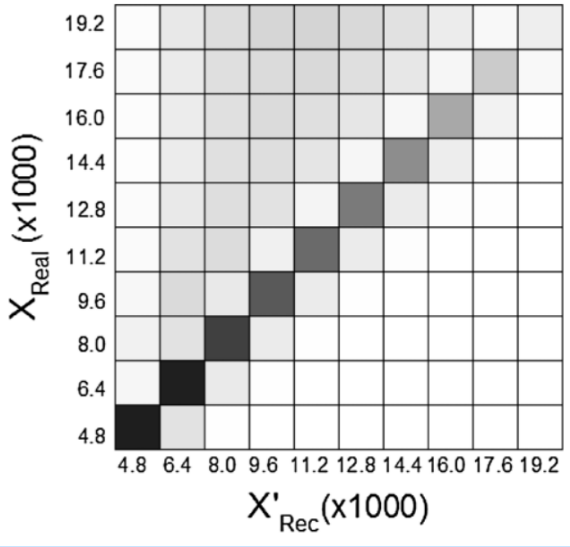

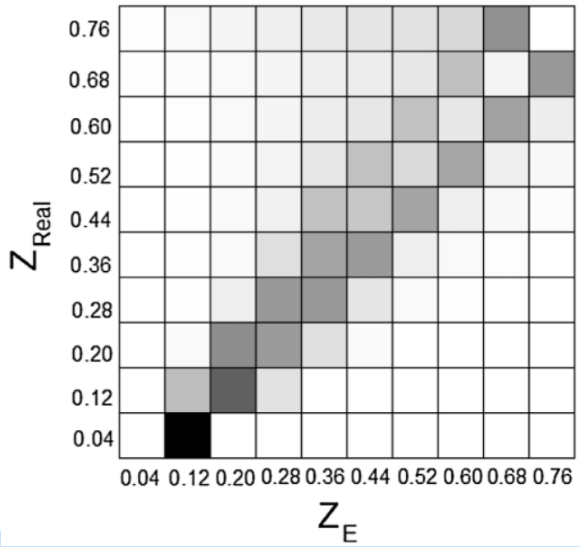

Reconstructing the partonic kinematics

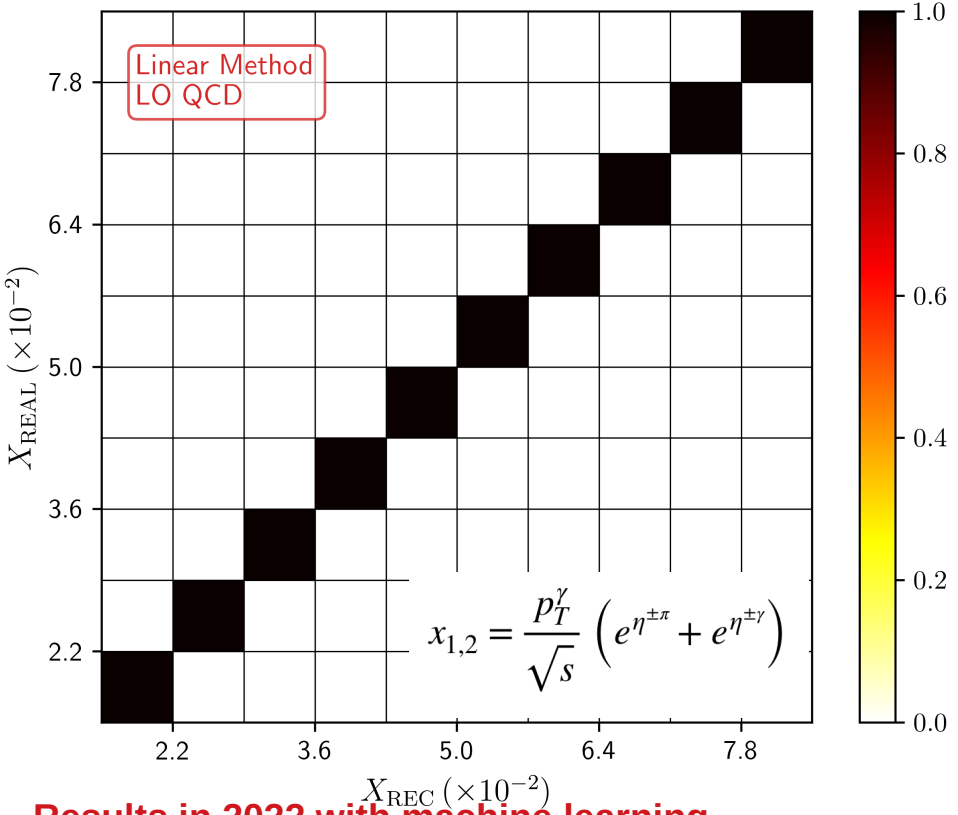

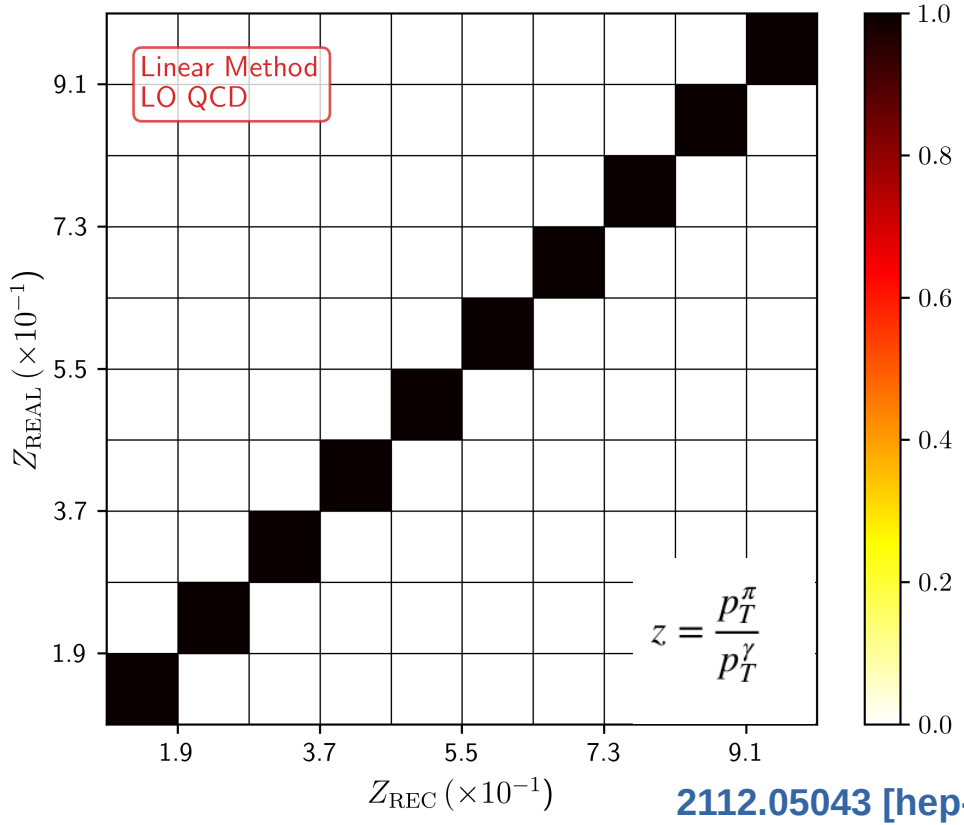

Results in 2022 with machine learning.

2112.05043 [hep-ph]

- **We started with LO cross-sections, and applied linear regression.**
- **We used the basis:** $\mathcal{B}_{\mathrm{LO}} = \{\frac{p_T^\gamma}{\sqrt{S_{CM}}}\exp(\eta^\pi),\ \frac{p_T^\gamma}{\sqrt{S_{CM}}}\exp(\eta^\gamma),\ \frac{p_T^\gamma}{\sqrt{S_{CM}}}\exp(-\eta^\pi),\ \frac{p_T^\gamma}{\sqrt{S_{CM}}}\exp(-\eta^\gamma),\ p_T^\pi/p_T^\gamma\}$

Reconstructions Methods

$$\mathrm{X} = \{ \mathrm{X}_{general}, X_{LO-ins}, X_{physically} \}$$

- **Linear Method**

$$\begin{aligned} Y_{REC} &= \sum_{i=k}^{i=0} \alpha_i x_i \text{ for } x_i \in X_j \\ j &= \text{general, LO-ins, physically} \end{aligned}$$

- **Gaussian Process Regression**

$$Y_{REC} = \prod_i \exp\left(-||x - \mu_i||^2 / 2l^2\right)$$

Reconstructions Methods

$$X = \{ X_{general}, X_{LO-ins}, X_{physically} \}$$

- **Linear Method**

$$Y_{REC} = \sum_{i=k}^{i=0} \alpha_i x_i \text{ for } x_i \in X_j$$

$$j = \text{general, LO-ins, physically}$$

- **Gaussian Process Regression**

$$Y_{REC} = \prod_i \exp\left(-||x - \mu_i||^2 / 2l^2\right)$$

- **Neural Network**

The NN implemented in this work is a **Multilayer Perceptron** with 5 hidden layers, 300 neurons per layer and a Relu (Unitary Linear Rectifier) activation function.

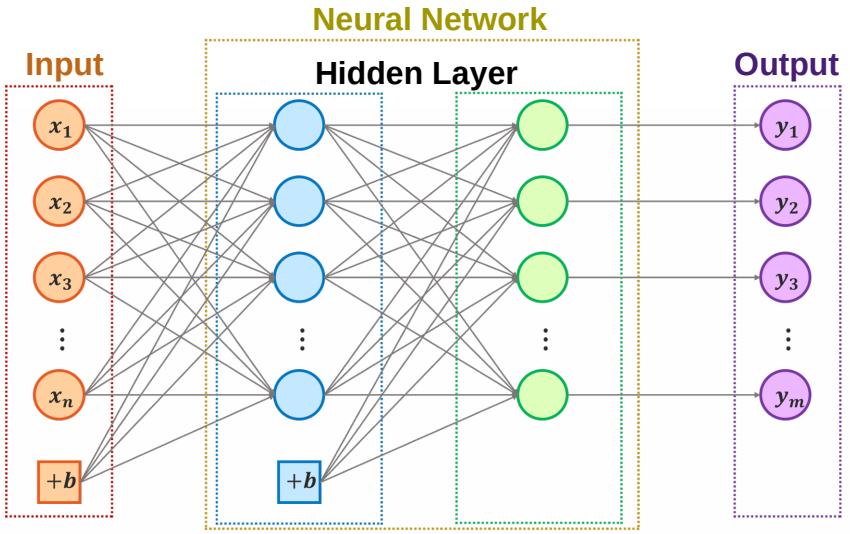

Input

$$\bar{\mathcal{V}}_{\text{Exp}} = \{\bar{p}_T^{\gamma}, \bar{p}_T^{\pi}, \bar{\eta}^{\gamma}, \bar{\eta}^{\pi}, \overline{\cos}(\phi^{\pi} - \phi^{\gamma})\}$$

Output

$\{x_1, x_2, z\}$

Reconstructing the partonic kinematics

General basis:

$$\mathcal{K} = \{\frac{p_T^\gamma}{\sqrt{S_{CM}}}, \frac{p_T^\pi}{\sqrt{S_{CM}}}, \exp(\eta^\gamma), \exp(\eta^\pi), \cos(\phi^\pi - \phi^\gamma), (\frac{p_T^\gamma}{\sqrt{S_{CM}}})^{-1}, (\frac{p_T^\pi}{\sqrt{S_{CM}}})^{-1}, (\exp(\eta^\gamma))^{-1}, (\exp(\eta^\pi))^{-1}\}$$

$$Y_{\rm REC} = \sum_{i=1, i\neq 5}^{9} (a_i^Y + b_i^Y\, \mathcal{K}_5)\, \mathcal{K}_i + \sum_{i\leq j, \{i,j\}\neq 5, j-i\neq 5} (c_{ij}^Y + d_{ij}^Y\, \mathcal{K}_5)\, \mathcal{K}_i \mathcal{K}_j$$

LO–inspired basis:

$$\mathcal{B}_{\rm NLO}^{X_1} = \{\frac{p_T^\gamma}{\sqrt{S_{CM}}}\exp(\eta^\gamma),\ \frac{p_T^\gamma}{\sqrt{S_{CM}}}\exp(\eta^\pi),\ \frac{p_T^\pi}{\sqrt{S_{CM}}}\exp(\eta^\gamma),\ \frac{p_T^\pi}{\sqrt{S_{CM}}}\exp(\eta^\pi),$$

$$\frac{p_T^\gamma \mathcal{K}_5}{\sqrt{S_{CM}}}\exp(\eta^\gamma),\ \frac{p_T^\gamma \mathcal{K}_5}{\sqrt{S_{CM}}}\exp(\eta^\pi),\ \frac{p_T^\pi \mathcal{K}_5}{\sqrt{S_{CM}}}\exp(\eta^\gamma),\ \frac{p_T^\pi \mathcal{K}_5}{\sqrt{S_{CM}}}\exp(\eta^\pi)\}$$

$$\mathcal{B}_{\rm NLO}^{Z} = \{p_T^\pi/p_T^\gamma,\ \mathcal{K}_5\, p_T^\pi/p_T^\gamma,\ \mathcal{K}_5\, p_T^\pi/\sqrt{S_{CM}},\ \mathcal{K}_5\, \sqrt{S_{CM}}/p_T^\gamma\}$$

Physically–motivated basis

$$x_{1,2} = \frac{p_T^\gamma}{\sqrt{s}}\left(e^{\eta^{\pm\pi}} + e^{\eta^{\pm\gamma}}\right) \qquad z = \frac{p_T^\pi}{p_T^\gamma}$$

$$b_6^{X_1} = 0\,,\quad c_{6,j}^{X_1} = d_{6,j}^{X_1} = c_{i,6}^{X_1} = d_{i,6}^{X_1} = 0 \quad \{i,j\} \in \{1,\ldots,9\}\,,$$

$$b_1^Z = b_7^Z = 0\,,\quad c_{1,j}^Z = d_{1,j}^Z = 0 \quad j \in \{1,\ldots,9\}\,, j \neq \{5,7\}\,,\quad c_{i,7}^Z = d_{i,7}^Z = 0 \quad i \in \{1,\ldots,9\}\,, i \neq \{1,5\}\,,$$

Reconstructing the partonic kinematics

2112.05043 [hep-ph]

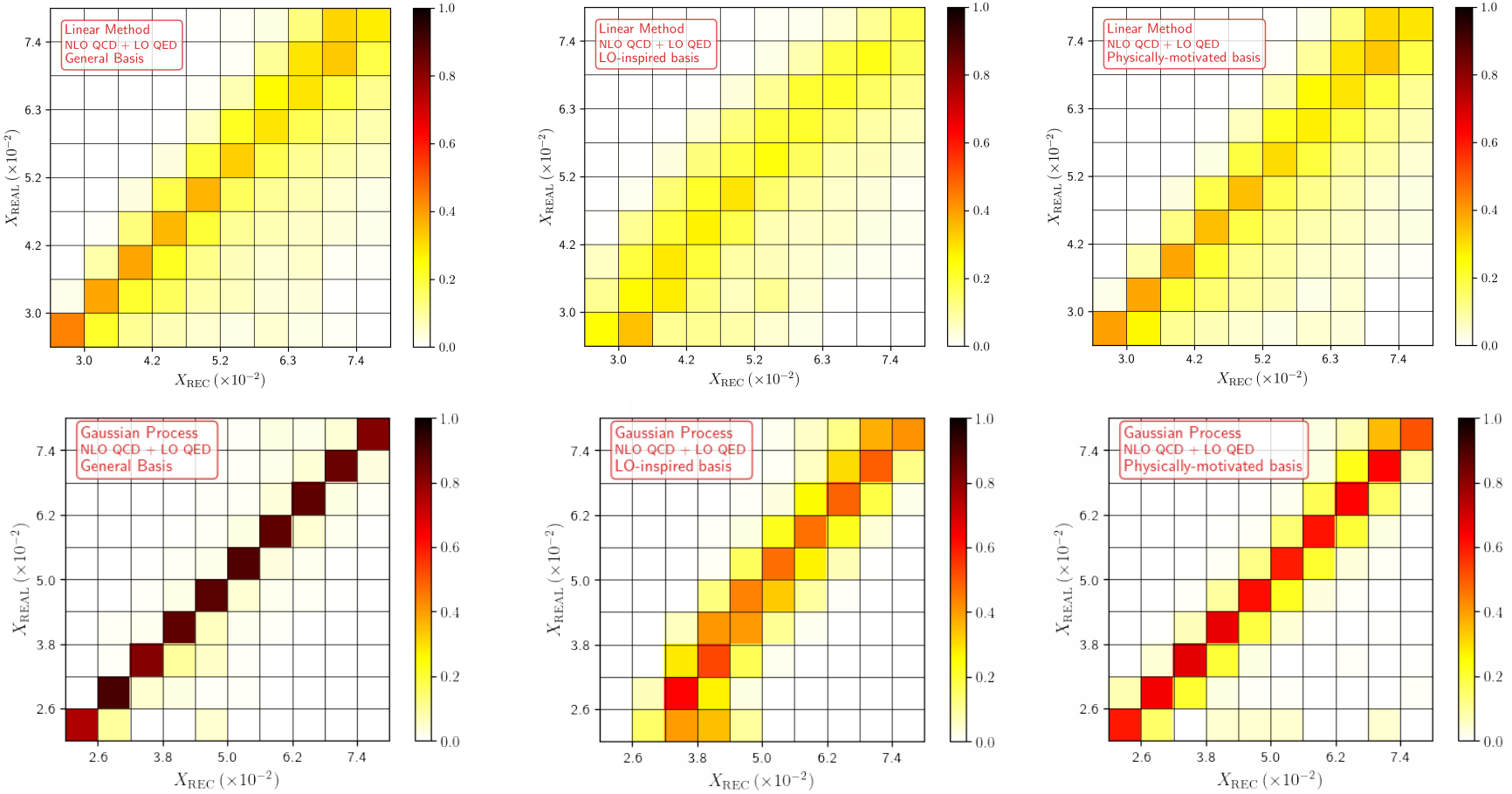

Reconstructing the partonic kinematics

2112.05043 [hep-ph]

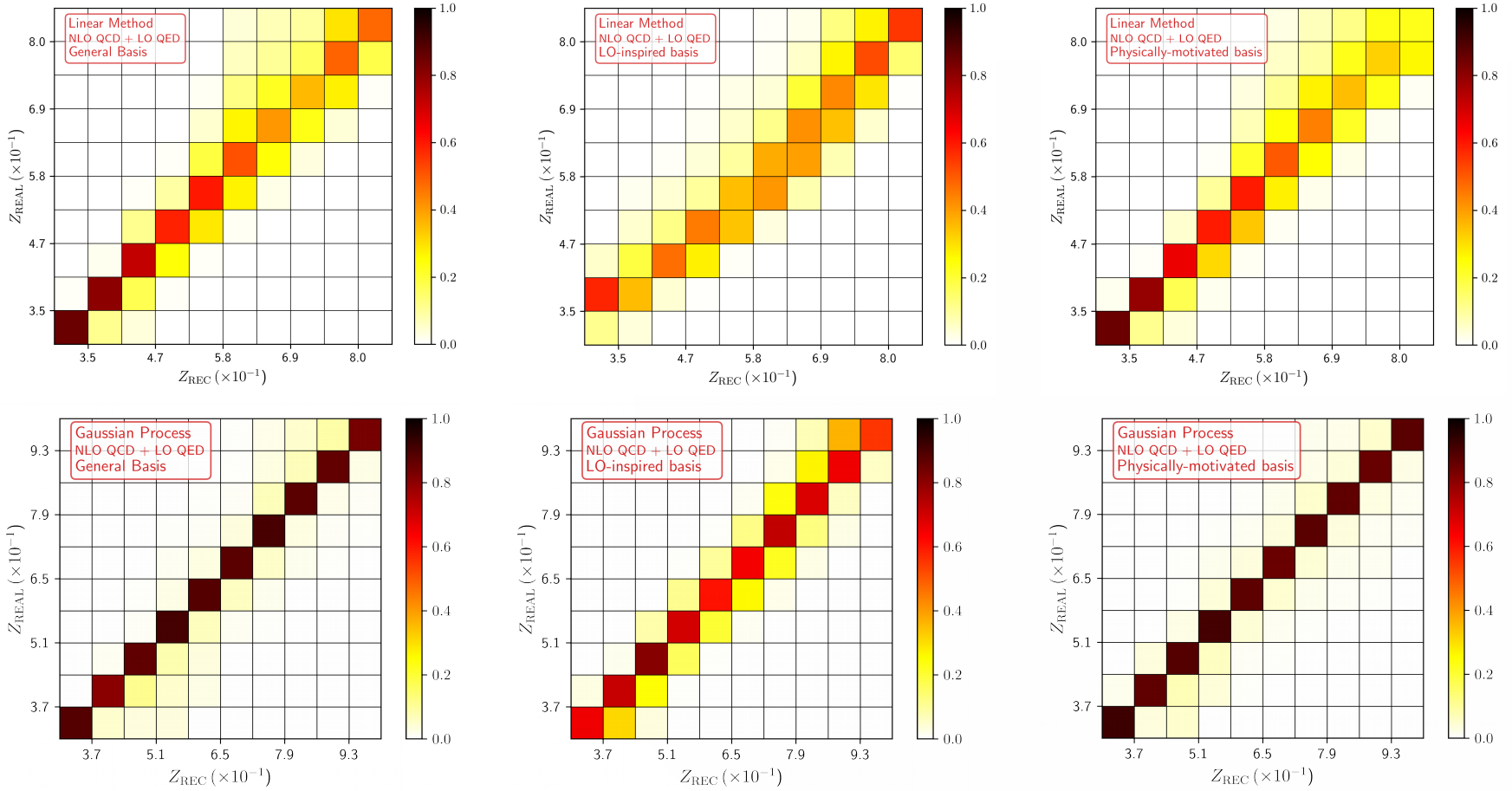

Reconstructing the partonic kinematics

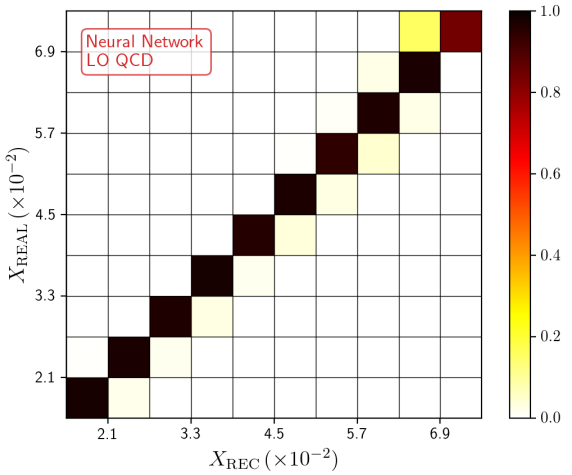

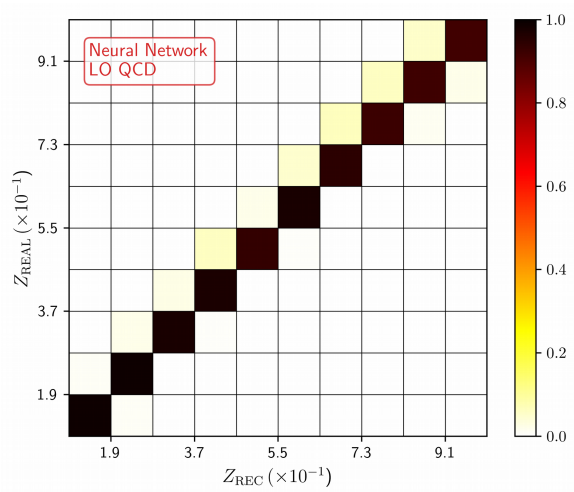

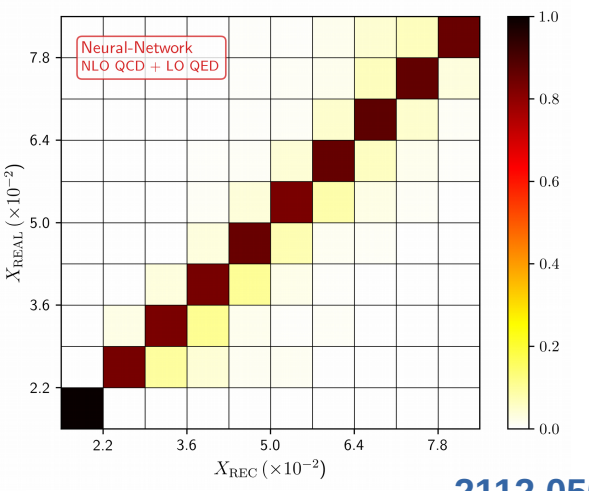

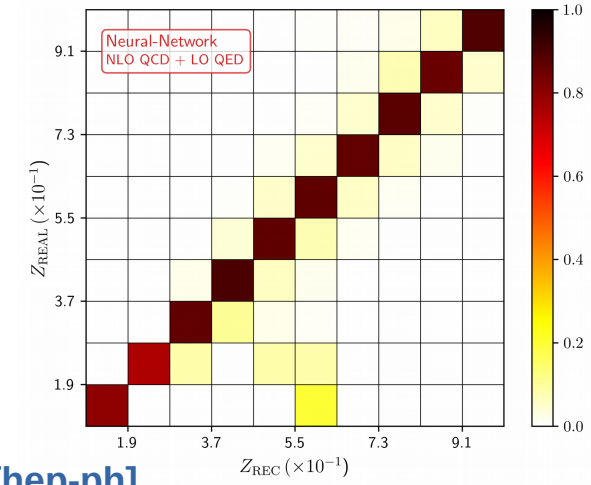

Neural Networks (NN) reconstruction

LO prediction

NLO QCD + LO QED prediction

2112.05043 [hep-ph]

Reconstructing the partonic kinematics

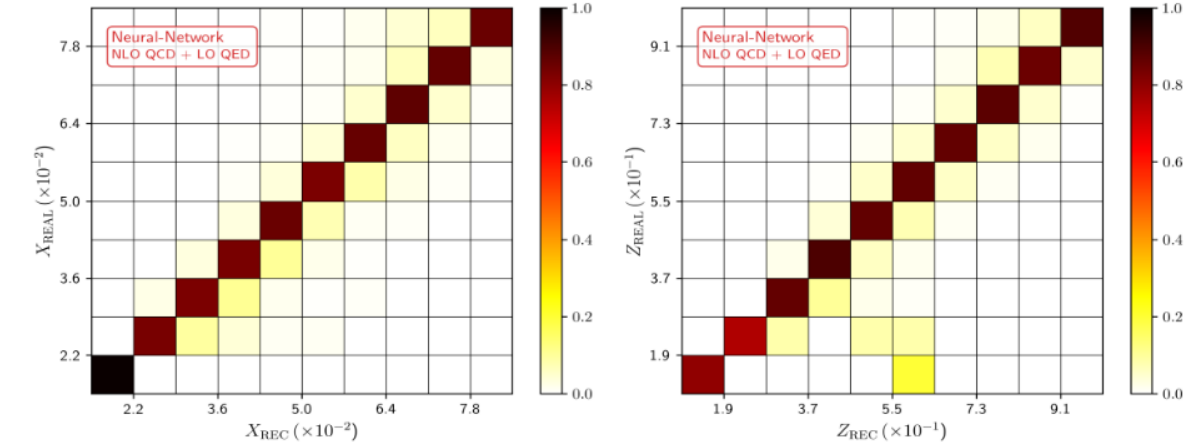

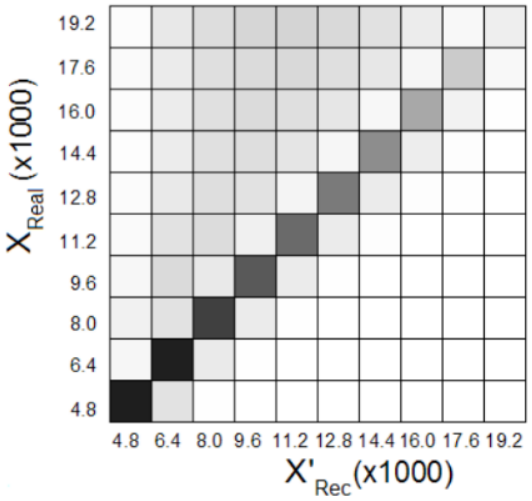

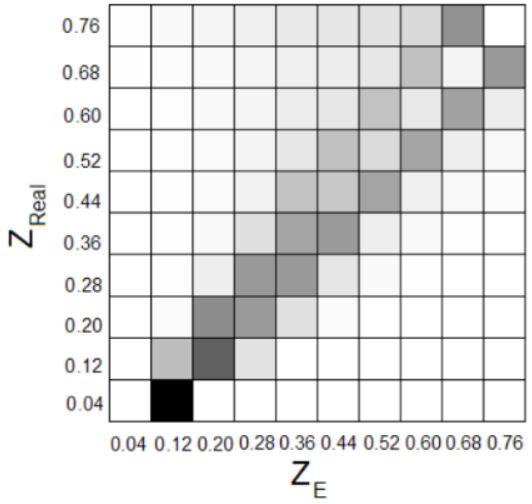

arXiv:2112.05043 [hep-ph]
Machine Learning
2022

arXiv:1011.0486 [hep-ph]
Analytical formula approx
2011

Conclusions

- Updated results are still consistent with ’11 analysis (modifications come from new PDFs and better FFs)
- LM: better for large-size basis
- GR: has more flexibility, and better agreement w.r.t. LM (improvement in X)
- NN: based on MLP, offers the best balance between assumptions and quality of the reconstruction

MLP techniques (specially NN) offers an outstanding framework to understand the partonic kinematics in an (almost) automatized and (almost) human-independent way


Thanks!

Reconstructing the partonic kinematics

Reconstructing {*x*, *z*} at higher-order

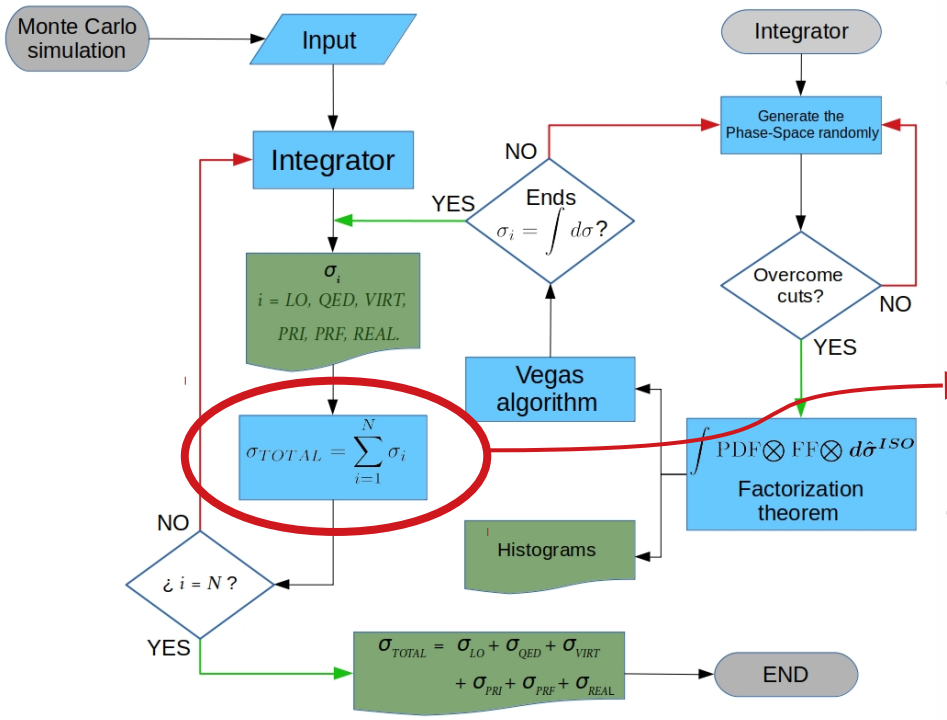

- NLO corrections involve: real (2-to-3), virtual (2-to-2), counterterms (2-to-2).

- Create “bins” in the external variables and compute the cross-section:

$$p_j = \{\bar{p}_T^{\gamma}, \bar{p}_T^{\pi}, \bar{\eta}^{\gamma}, \bar{\eta}^{\pi}, \overline{\cos}(\phi^{\pi} - \phi^{\gamma})\} \in \bar{\mathcal{V}}_{\mathrm{Exp}}$$

$$\sigma_j(\bar{p}_T^{\gamma}, \bar{p}_T^{\pi}, \bar{\eta}^{\gamma}, \bar{\eta}^{\pi}, \overline{\cos}(\phi^{\pi} - \phi^{\gamma})) = \int_{(p_T^{\gamma})_{j,\mathrm{MIN}}}^{(p_T^{\gamma})_{j,\mathrm{MAX}}} dp_T^{\gamma} \int_{(p_T^{\pi})_{j,\mathrm{MIN}}}^{(p_T^{\pi})_{j,\mathrm{MAX}}} dp_T^{\pi} \ldots \times \int dx_1 dx_2 dz \, d\bar{\sigma}$$

- Weight the MC momentum fractions with the cross-section per bin:

$$(x_1)_j = \sum_i (x_1)_i \frac{d\sigma_j}{dx_1}(p_j; (x_1)_i)$$

$$(z)_j = \sum_i z_i \frac{d\sigma_j}{dz}(p_j; z_i)$$

Motivation

- Aim: reconstruct the momentum fractions x_1, x_2 and z.

- Nowadays, Machine Learning is a tool that allows to make a predictive model to reconstruct $\{x_1, x_2, z\}$.

2104.14663

Analysis of the internal structure of hadrons using direct photon production

David F. Rentería-Estrada,[a] Roger J. Hernández-Pinto[a] and German F. R. Sborlini[b,c]

loa, Ciudad Universi-

ien, Germany.
ior de Investigaciones

1011.0486

PHYSICAL REVIEW D **83,** 074022 (2011)

Hadron plus photon production in polarized hadronic collisions at next-to-leading order accuracy

Daniel de Florian and Germán F. R. Sborlini

Departamento de Física Facultad de Ciencias Exactas y Naturales, Universidad de Buenos Aires Pabellón I, Ciudad Universitaria (1428) Capital Federal, Argentina

(Received 3 November 2010; revised manuscript received 23 February 2011; published 27 April 2011)

We compute the next-to-leading order QCD corrections to the polarized (and unpolarized) cross sections for the production of a hadron accompanied by an opposite-side prompt photon. This process, being studied at RHIC, permits us to reconstruct partonic kinematics using experimentally measurable variables. We study the correlation between the reconstructed momentum fractions and the true partonic ones, which in the polarized case might allow us to reveal the spin-dependent gluon distribution with a higher precision.

DOI: 10.1103/PhysRevD.83.074022 PACS numbers: 13.88.+e, 12.38.Bx, 13.87.Fh

2112.05043

Reconstructing partonic kinematics at colliders with Machine Learning

of hadrons is a hard
is starting from first
is necessary to use
article, we describe
. Using up-to-date
orrections to hadron

D. F. Rentería-Estrada,[a] R. J. Hernández-Pinto,[a] G. F. R. Sborlini[b,c] and P. Zurita[d]

[a] *Facultad de Ciencias Físico-Matemáticas, Universidad Autónoma de Sinaloa, Ciudad Universitaria, CP 80000 Culiacán, Mexico*

[b] *Instituto de Física Corpuscular, Universitat de València – Consejo Superior de Investigaciones Científicas, Parc Científic, E-46980 Paterna, Valencia, Spain*

[c] *Deutsches Elektronen-Synchrotron DESY, Platanenallee 6, 15738 Zeuthen, Germany*

[d] *Institut für Theoretische Physik, Universität Regensburg, 93040 Regensburg, Germany, Universität Regensburg, Germany*

E-mail: davidrenteria.fcfm@uas.edu.mx, roger@uas.edu.mx, german.sborlini@desy.de, maria.zurita@ur.de

2011 **2021**

Photon + Hadron correlations

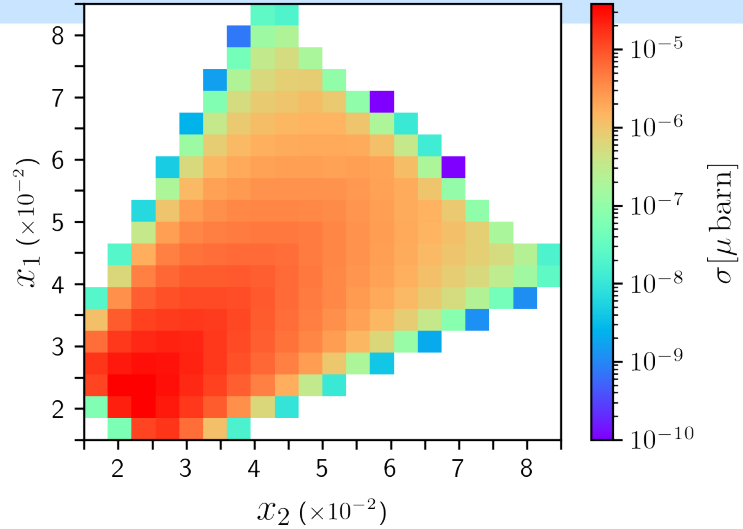

LO QCD

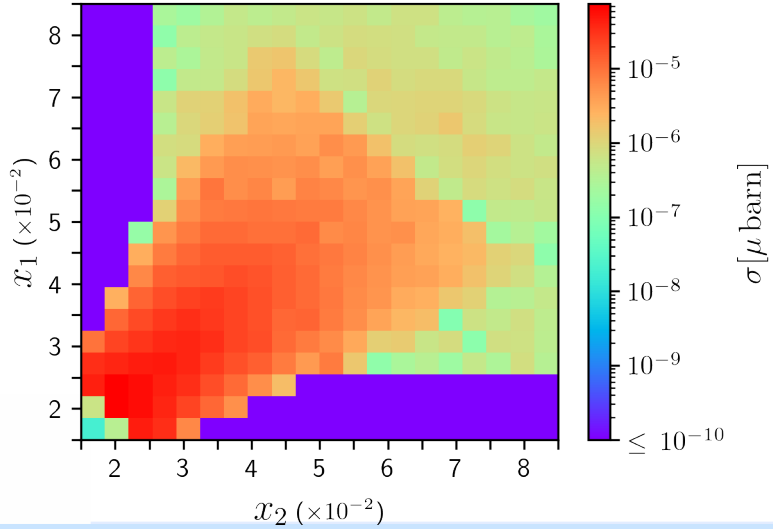

NLO QCD + LO QED

- Positive correlation
- Consequence of the initial state symmetry (pp collision)
- It is a cross-check

This procedure leads to three functions for reconstructing each momentum fraction: given a kinematic point in the grid, $p_j \in \bar{\mathcal{V}}_{\rm Exp}$, we have

$$X(p_j) \equiv \{X_{\rm REC}^{(\xi=2)}(p_j), X_{\rm REC}^{(\xi=1)}(p_j), X_{\rm REC}^{(\xi=1/2)}(p_j)\}, \tag{50}$$

and define

$$X_{\rm REC}(p_j) = \overline{X(p_j)} \pm \frac{\max(X(p_j)) - \min(X(p_j))}{2} \equiv \overline{X(p_j)} \pm \Delta X(p_j)\,, \tag{51}$$

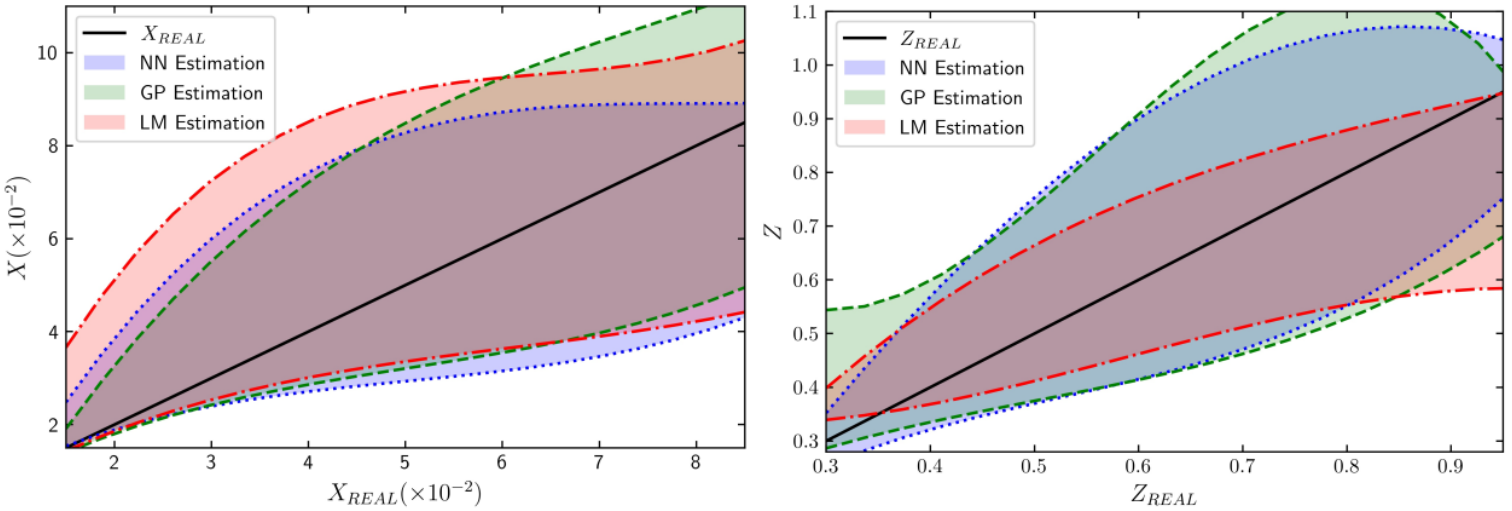

Parameters	TEST 1	TEST 2	TEST 3
# hidden layers	2	4	3
# neurons/layer	50	100	100
tolerance	10^{-2}	10^{-2}	10^{-3}
max. number of iterations	10^{8}	10^{8}	10^{9}
# iterations w/o change	14,000	21,000	100,000

Table 3: Architectures for the MLP of three different tests for the reconstruction of the momentum fractions at NLO in QCD. All parameters are taken to be the same for X_{REC} and Z_{REC}.

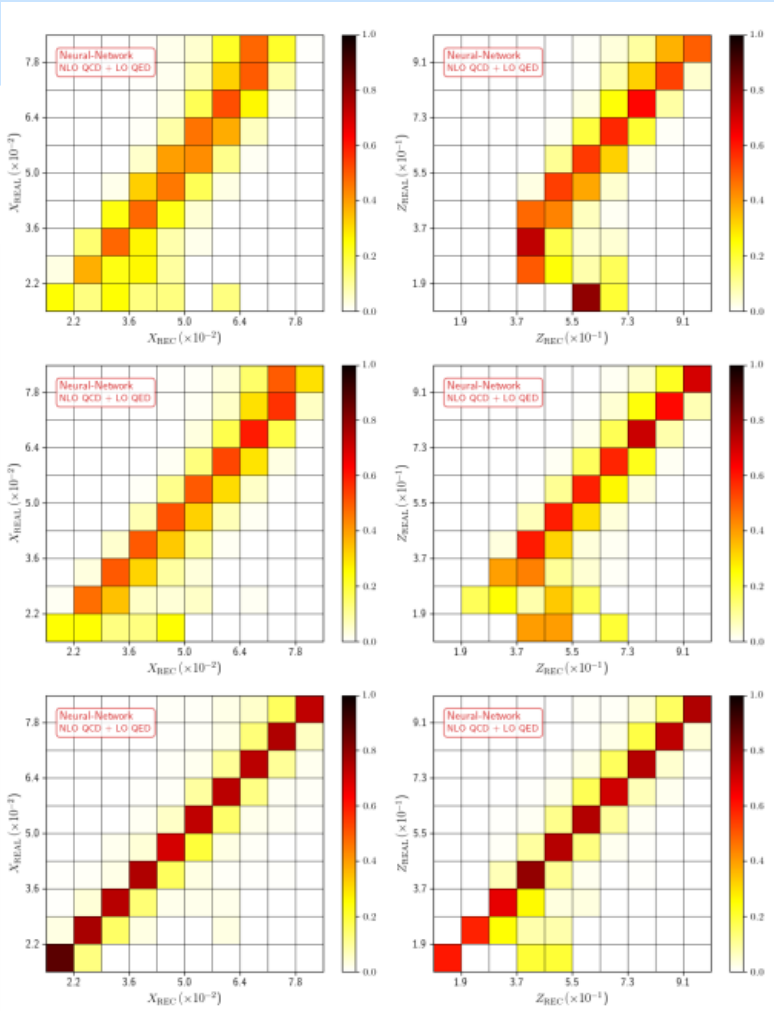

Figure 19: Comparison of the momentum fractions X_{REAL} vs. X_{REC} (left) and Z_{REAL} vs. Z_{REC} (right) obtained with MLP at NLO QCD + LO QED accuracy. The parameters for TEST1 (upper row), TEST2 (middle row) and TEST3 (lower row) are given in Table 3.

	X_{REC} (LO)	Z_{REC} (LO)	X_{REC} (NLO)	Z_{REC} (NLO)
# of hidden layers	2	1	5	5
# of neurons/layer	200	100	300	300
activation function	ReLU	ReLU	ReLU	ReLU
# iterations	1×10^5	1×10^5	1×10^{12}	1×10^{12}
learning rate	1×10^{-3}	1×10^{-3}	1×10^{-4}	1×10^{-4}

Table 2: Architecture for the MLP best fit parameters for the reconstruction of the momentum fractions at LO in QCD: $X_{\rm REC}$(LO) and $Z_{\rm REC}$(LO) (second and third columns), and for the momentum fractions at NLO QCD + LO QED: $X_{\rm REC}$(NLO) and $Z_{\rm REC}$(NLO) (fourth and fifth columns).

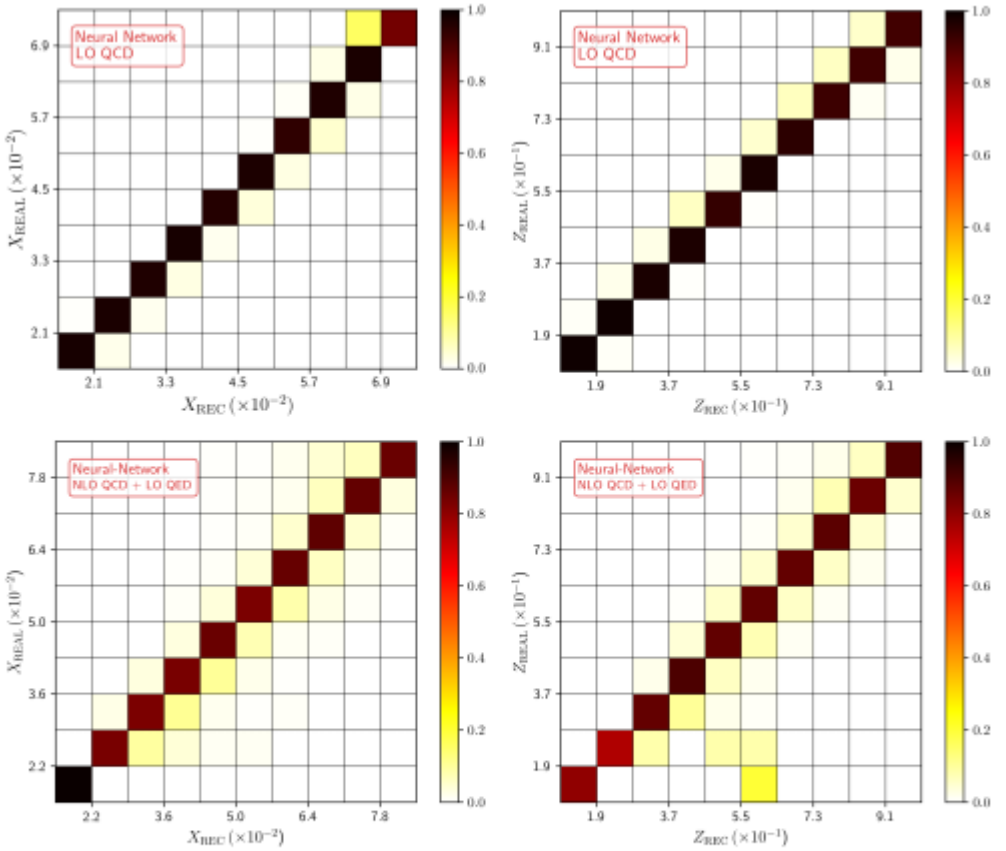

Figure 15: Left: Comparison of the momentum fractions $X_{\rm REAL}$ and $X_{\rm REC}$ obtained with MLP neural networks with the parameters given in Table 2. The upper (lower) row corresponds to the LO QCD (NLO QCD + LO QED) data set. Right: same as the l.h.s but for $Z_{\rm REAL}$ and $Z_{\rm REC}$.

Reconstructing the partonic kinematics

Reconstructing {*x*, *z*} at higher-order

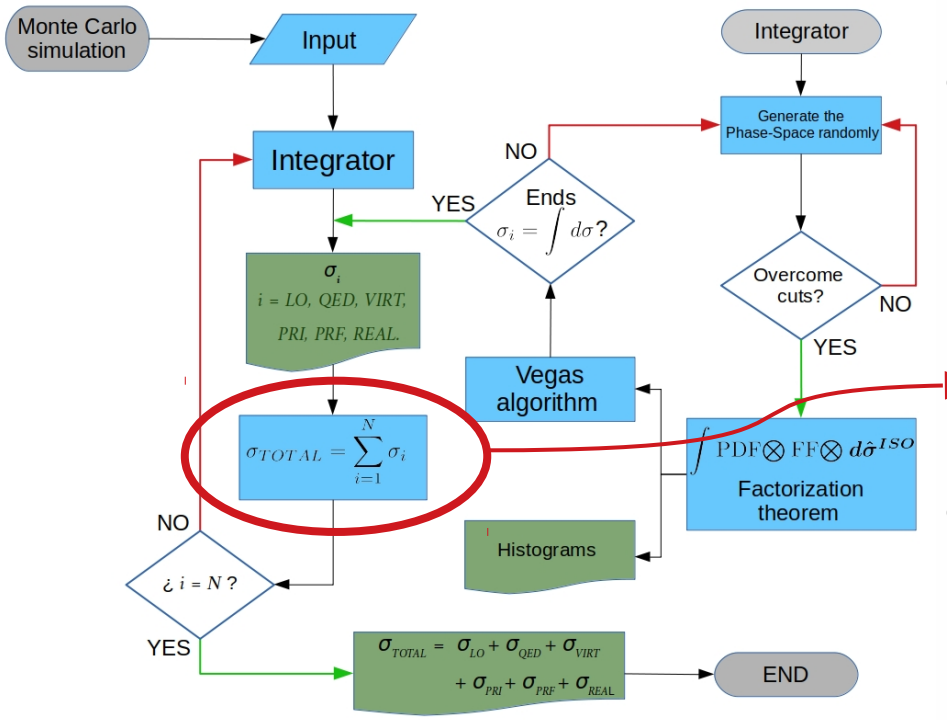

- NLO corrections involve: real (2-to-3), virtual (2-to-2), counterterms (2-to-2).
- Create “bins” in the external variables and compute the cross-section:

$$p_j = \{\bar{p}_T^{\gamma}, \bar{p}_T^{\pi}, \bar{\eta}^{\gamma}, \bar{\eta}^{\pi}, \overline{\cos}(\phi^{\pi} - \phi^{\gamma})\} \in \bar{\mathcal{V}}_{\mathrm{Exp}}$$

$$\sigma_j(\bar{p}_T^{\gamma}, \bar{p}_T^{\pi}, \bar{\eta}^{\gamma}, \bar{\eta}^{\pi}, \overline{\cos}(\phi^{\pi} - \phi^{\gamma})) = \int_{(p_T^{\gamma})_{j,\mathrm{MIN}}}^{(p_T^{\gamma})_{j,\mathrm{MAX}}} dp_T^{\gamma} \int_{(p_T^{\pi})_{j,\mathrm{MIN}}}^{(p_T^{\pi})_{j,\mathrm{MAX}}} dp_T^{\pi} \ldots \times \int dx_1 dx_2 dz \, d\bar{\sigma}$$

- Weight the MC momentum fractions with the cross-section per bin:

$$(x_1)_j = \sum_i (x_1)_i \frac{d\sigma_j}{dx_1}(p_j; (x_1)_i)$$

$$(z)_j = \sum_i z_i \frac{d\sigma_j}{dz}(p_j; z_i)$$

Second: Photon + Hadron correlations

LO kinematics

- x vs p_T

$$x_{1,2} = \frac{p_T^{\gamma}}{\sqrt{s}}\left(e^{\eta^{\pm\pi}} + e^{\eta^{\pm\gamma}}\right)$$

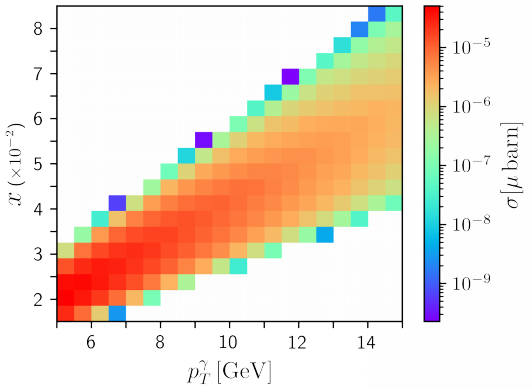

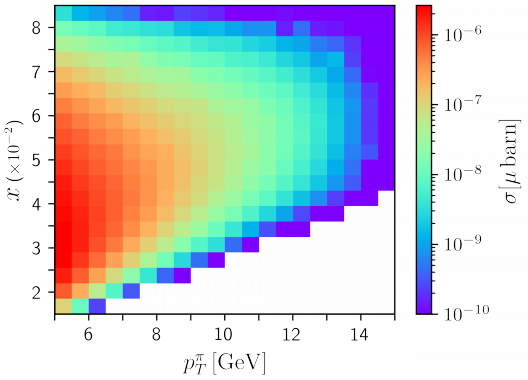

- z vs p_T

$$z = \frac{p_T^{\pi}}{p_T^{\gamma}}$$

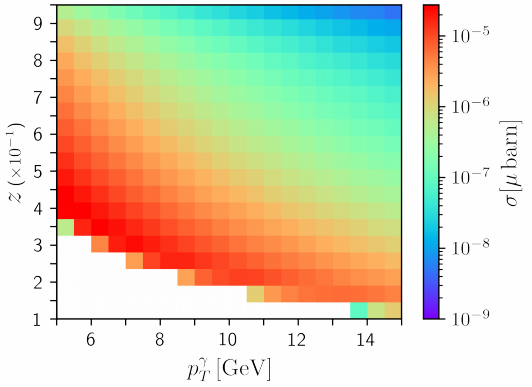

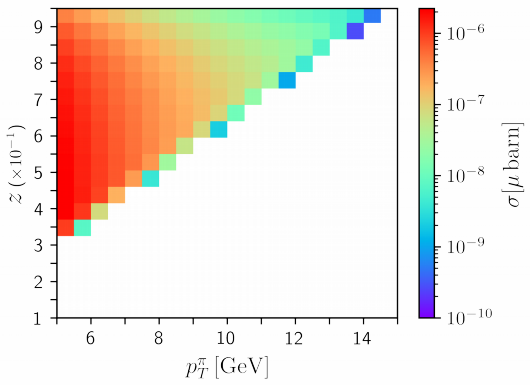

Second: Photon + Hadron correlations

NLO kinematics

- x vs p_T

$$x_{1,2} = ?$$

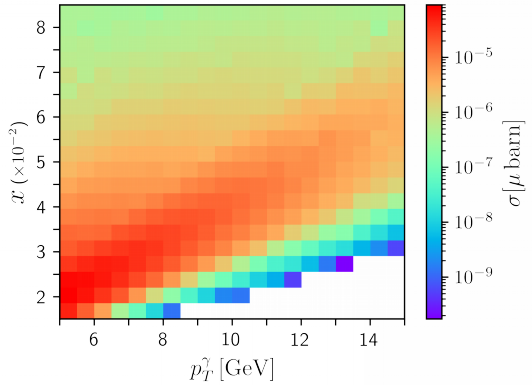

- z vs p_T

$$z = ?$$